Soft Matter

PAPER

View Article Online
View Journal | View Issue

Cite this: *Soft Matter*, 2015, **11**, 2852

Destabilisation of the hexatic phase in systems of hard disks by quenched disorder due to pinning on a lattice

Weikai Qi and Marjolein Dijkstra*

Received 24th December 2014
Accepted 11th February 2015

DOI: 10.1039/c4sm02876g

www.rsc.org/softmatter

We investigate the effect of quenched disorder on the melting mechanism of two-dimensional hard disks using large-scale event-driven molecular dynamics simulations. The two-stage melting scenario of a continuous solid–hexatic and a first-order hexatic–liquid transition for a 2D system of hard disks does *not* persist in the case of quenched disorder, which arises by pinning less than one percent of the particles on a triangular lattice. Based on the Halperin–Nelson–Young (HNY) renormalization group equation, we observe that a first-order solid–liquid transition preempts the Kosterlitz–Thouless-type solid–hexatic transition in a 2D system of hard disks with quenched disorder as the stiffness of the crystal is increased by the presence of pinned particles.

I. Introduction

According to the Kosterlitz–Thouless–Halperin–Nelson–Young (KTHNY) theory, the melting mechanism of a 2D crystal proceeds *via* two consecutive continuous transitions, which are induced by unbinding of topological defects.[1–3] A 2D crystal melts *via* dissociation of dislocation pairs into an intermediate hexatic phase. The hexatic phase is characterized by short-ranged positional order, but quasi-long-ranged bond orientational order.[4–6] Subsequently, the hexatic phase transforms into a liquid with short-ranged positional and orientational order *via* the unbinding of dislocations into free disclinations.[1–3]

Many simulation and experimental studies have been carried out to investigate the melting mechanism of a 2D solid, thereby providing support for both two-stage melting scenarios *via* an intermediate hexatic phase as well as a first-order melting transition.[7–12] These results seem to suggest that 2D melting depends sensitively on the particle interactions, out-of-plane fluctuations, and finite-size effects. Even in the simple case of a 2D system of hard disks, conflicting results have been obtained.[13–25] However, recent simulation studies showed, in contrast to predictions of the KTHNY theory, that systems of hard disks melt *via* a first-order liquid–hexatic phase transition and a continuous hexatic–solid transition.[26,27] These results settled a long-standing debate on the 2D melting scenario of hard disks.

From an experimental point of view, there is, however, still no consensus on the nature of the 2D melting transition. Even for particle systems interacting *via* short-range repulsive pair potentials conflicting results have been found experimentally.[8,10,28] Therefore, it remains essential to investigate in more detail about the origin of the conflict between the various experimental observations. In most experiments on 2D melting, colloidal particles were confined between two glass plates.[8,10,28–31] Two main factors in these experiments may alter the melting scenario from that of a strictly 2D system, *i.e.*, out-of-plane motion of the particles and quenched disorder due to pinning of particles by confinement. Regarding the out-of-plane fluctuations, a recent simulation study showed that the two-step melting scenario as observed for 2D hard disks is not altered in the case of a quasi-2D monolayer of hard spheres with out-of-plane motions as large as half the diameter of the spheres.[32] In the case of quenched disorder, a random fraction of particles can be pinned either to random positions in the system or on lattice sites of an underlying crystal phase. With regard to pinned particles at random sites, it was shown theoretically that the KTHNY melting scenario persists, and that the solid phase is destroyed entirely for high pinning fractions resulting in a hexatic glass.[33–37] Experiments and simulations on 2D melting of super-paramagnetic colloidal particles with quenched disorder confirmed the increased stability range of the hexatic phase.[38] In this study, we investigate the melting of a 2D system of hard disks with quenched disorder, which results by pinning random particles on a crystal lattice. We find that the two-step melting mechanism of a 2D system of hard disks changes by pinning particles on a lattice. More precisely, we show that the hexatic phase is destabilized and that a first-order solid–liquid phase transition preempts the Kosterlitz–Thouless-type solid–hexatic transition. Thus our results show that quenched disorder due to pinning of particles on a lattice leads to a different melting scenario than in the case of pinning at random positions.

Soft Condensed Matter, Debye Institute for Nanomaterials Science, Utrecht University, Princetonplein 5, 3584 CC Utrecht, The Netherlands. E-mail: M.Dijkstra1@uu.nl

II. Model and simulation methods

We investigate the melting mechanism of a 2D system of $N = 1024^2 = 1\,048\,576$ hard disks of diameter σ in the presence of pinned particles using event-driven molecular dynamics (EDMD) simulations in the NVT ensemble with V the volume and T the temperature. In an EDMD simulation, the system evolves *via* elastic collision events, which are described by Newton's equations of motion. The collisions are perfectly elastic, *i.e.*, energy and momentum are preserved. In addition, we employed an event calendar to maintain a list of all particle collisions. In the simulations, we started from a perfect lattice and quenched disorder is introduced by pinning randomly chosen particles with a fraction q_d to the sites on a triangular commensurable lattice. For sufficiently high pinning fractions, the solid phase exhibits long-ranged positional order, whereas for low pinning fractions, the positional order in the solid phase is quasi-long ranged. The simulation times of all our runs were 2000τ corresponding to about 2×10^{10} displacements, with $\tau = \sqrt{m\sigma^2/k_BT}$ and $m = 1$ being the mass of the particles. After such a long equilibration time, we find that the pressure reaches a plateau as a function of time and that the statistical fluctuations in the pressure are very small, thereby lending support that our simulations are equilibrated.

We compute the reduced pressure $P^* = \beta P\sigma^2$ from the collision rate *via* the virial theorem given by

$$P^* = \frac{N\sigma^2}{A}\left[1 - \frac{\beta m}{2t}\frac{1}{N}\sum \mathbf{r}_{ij}\cdot\mathbf{v}_{ij}\right], \quad (1)$$

where $A = L_xL_y$ is the area, m is the mass of the particles, t is the time interval, $\mathbf{r}_{ij}$ and $\mathbf{v}_{ij}$ are the distance and velocity vectors, respectively, between particles i and j.

III. Results

A. Equation of state

In Fig. 1, we plot the reduced pressure P^* as a function of the area fraction $\eta = \pi N\sigma^2/4A$ for varying pinning fractions $0 \leq q_d \leq 0.01$. We checked our results for $N = 1024^2$ particles with those obtained for $N = 128^2$, but averaged over 16 different realizations of randomly pinned particles. We find good agreement within our statistical accuracy. For all q_d considered, we observe a Mayer–Wood loop in the equation of state due to interfacial tension effects on finite systems.[39] We determine the coexisting densities using a Maxwell construction to the equation of state, and plot the phase boundaries in Fig. 2. The clear presence of a Mayer–Wood loop in the equation of state lends strong support for a first-order phase transition.[26] We clearly observe from Fig. 2 that the first-order phase transition shifts to lower area fractions η upon increasing the pinning fraction q_d. We have calculated the latent heat per particle L/N for the first-order phase transition using $L/N = p_{coex}(1/\rho_f - 1/\rho_s)$ with p_{coex} the bulk coexistence pressure, and ρ_f and ρ_s the bulk density of the coexisting fluid and solid (hexatic) phase. The result is shown in Fig. 3. The latent heat L increases with pinning fraction q_d, and we find that the slope of the latent heat L changes at $q_d = 0.0035$ where the fluid–hexatic phase coexistence becomes unstable with respect to the fluid–solid phase coexistence.

B. Subblock scaling analysis

Subsequently, we turn our attention to the positional and bond orientational order of the coexisting phase at a high density. To this end, we perform a sub-block scaling analysis of the 2D positional order parameter in reciprocal space

$$\Psi_{\mathbf{G}} = \left|\frac{1}{N}\sum_{i=1}^{N}\exp(i\mathbf{G}\cdot\mathbf{r}_i)\right|^2, \quad (2)$$

where the sum runs over all particles i, $\mathbf{r}_i$ is the position of particle i and $\mathbf{G}$ denotes the wave vector that corresponds to a diffraction peak and equals $2\pi/a$ with a the averaged interparticle distance as determined by taking the value of a that maximizes $\Psi_{\mathbf{G}}$. In the solid phase, the averaged particle distance equals the averaged lattice spacing, which is corrected for the presence of vacancies and other defects.[26] In addition, we calculated $\Psi_{\mathbf{G}}$ for varying sub-block sizes L_b/L with

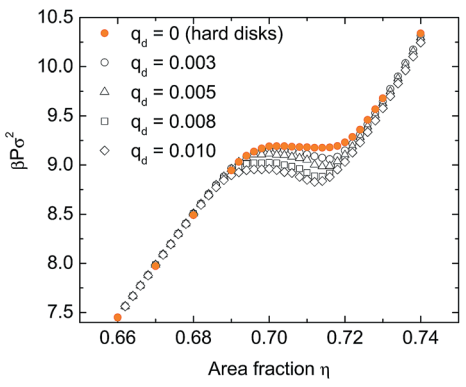

Fig. 1 Reduced pressure $P^* = \beta P\sigma^2$ as a function of area fraction $\eta = \pi N\sigma^2/4A$ for $N = 1024^2$ hard disks with diameter σ and area $A = L_xL_y$ for varying pinning fractions q_d. From top to bottom the pinning fraction q_d is 0 (pure hard disks), 0.003, 0.005, 0.008 and 0.01, respectively.

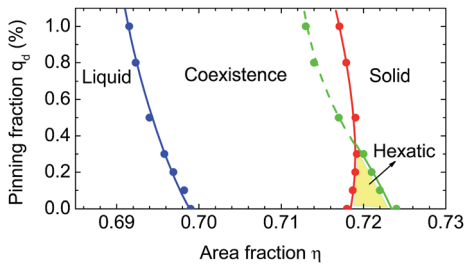

Fig. 2 Phase diagram of a system of hard disks subject to quenched disorder due to pinned particles on a crystal lattice in the area fraction η *versus* pinning fraction q_d representation. The blue and red dots denote the liquid and solid binodal, respectively. The green dots correspond to a continuous solid–hexatic phase transition, which was calculated from a finite-size scaling analysis of the positional order. All lines are guides to the eye. The dashed part of the green line indicates that the hexatic phase is metastable with respect to a first-order liquid–solid phase transition.

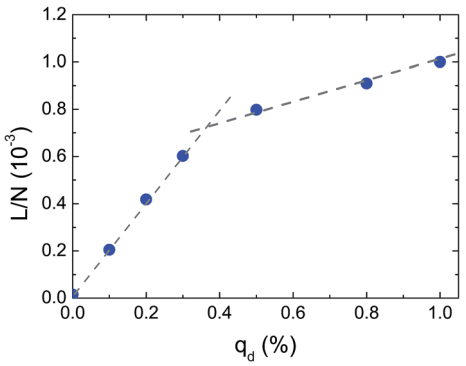

Fig. 3 The latent heat L/N for $N = 1024^2$ hard disks as a function of quenched disorder q_d. Dashed lines are linear fittings of the data for $q_d > 0.0035$ and $q_d < 0.0035$.

$L = \sqrt{L_x L_y}/4$ and analyzed the scaling of $\ln(\Psi_G(L_b)/\Psi_G(L))$ *versus* $\ln(L_b/L)$. The statistical averaging was performed by dividing the system into 64 subsystems, which yielded satisfactory statistics. According to the KTHNY theory, the positional order parameter is expected to decay algebraically, *i.e.*, $\Psi_G(L) \propto L^{-\alpha}$ with an exponent $0 \leq \alpha \leq \eta_t$ in the solid phase, while in the liquid and hexatic phase the positional order decays exponentially, and thus a plot of $\ln(\Psi_G(L))$ *versus* $\ln(L)$ should show a slope of -2 for sub-block sizes larger than the bulk correlation length in the liquid phase.[40] According to the KTHNY theory, η_t is 1/3, which should not be affected by quenched disorder.[33] In the case of pure hard disks, *i.e.*, without any pinning effects, a first-order fluid–hexatic phase transition with coexisting densities $\eta_L = 0.700$ and $\eta_H = 0.716$ of the liquid and hexatic phase, respectively, and a continuous hexatic–solid transition at $\eta_{HS} \simeq 0.724$ were observed.[26,27] These results were confirmed by a sub-block scaling analysis in ref. 32. In Fig. 4, we show the sub-block scaling analysis for a system of hard disks with a pinning fraction $q_d = 0.005$. Fig. 4 shows that the positional order decays algebraically with a slope $\alpha < 1/3$ for $\eta \geq 0.716$. We thus find a continuous hexatic–solid phase transition at an area fraction

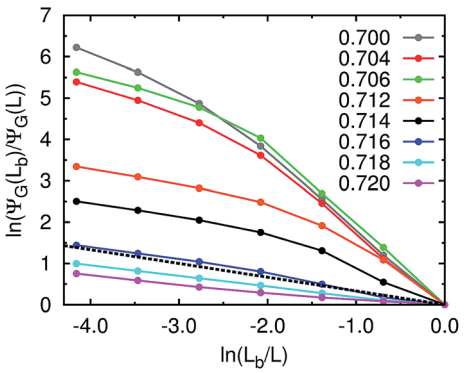

Fig. 4 Sub-block scaling analysis of the 2D positional order parameter in reciprocal space $\Psi_G(L_b)$ *versus* L_b for hard disks with a pinning fraction $q_d = 0.005$ for varying area fractions η as labeled. The slope of the black dashed lines corresponds to $-1/3$, which indicates a continuous hexatic–solid transition according to the KTHNY theory.

$\eta \simeq 0.716$, which lies well-inside the solid–liquid coexistence region as determined from a Maxwell construction to the equation of state. Hence, the hexatic phase is pre-empted by a first-order fluid–solid transition by the presence of pinned particles.

Employing the same analysis as described above for other values of q_d, we find that a stable hexatic phase persists only in the range of pinning fractions $0 \leq q_d \leq 0.003$. For $q_d > 0.003$, we did not observe a stable hexatic phase. In Fig. 2, we show the resulting phase diagram of hard disks subject to quenched disorder due to pinned particles on a lattice. We find that the coexisting densities of the liquid and solid phase decrease upon increasing the pinning fraction q_d. Moreover, our results show that the hexatic phase is preempted by a first-order fluid–solid transition for sufficiently high pinning fractions q_d. Our findings contrast the results for the case of quenched disorder due to particles pinned at random sites, where the density regime of the hexatic phase enlarges upon increasing q_d.[35–37] We thus find that pinning particles at random positions destabilizes the solid and stabilizes the hexatic phase, whereas pinning particles on random positions of a crystal lattice stabilizes the solid phase and destroys the hexatic phase.

IV. Renormalization group analysis

To corroborate our results, we also perform a renormalization group analysis based on the KTHNY theory.[1–3] According to the KTHNY theory, a solid–hexatic phase transition occurs when the Young's modulus

$$K = \frac{4\mu(\mu+\lambda)}{2\mu+\lambda}\frac{2}{\sqrt{3}\rho k_B T} = 16\pi, \tag{3}$$

where λ and μ are the 2D shear and bulk Lamé elastic constants and ρ the density. This melting criterion is not affected by quenched disorder.[33] However, due to the presence of dislocations, which have a fluid-like response to the stress, the Young's modulus K should be renormalized as described by the KTHNY renormalization group recursion relationships[2,3]

$$\frac{dK^{-1}(l)}{dl} = \frac{3}{4}\pi y^2(l) e^{\frac{K(l)}{8\pi}}\left[2I_0\left(\frac{K(l)}{8\pi}\right) - I_1\left(\frac{K(l)}{8\pi}\right)\right],$$

$$\frac{dy}{dl} = \left(2 - \frac{K(l)}{8\pi}\right)y(l) + 2\pi y^2(l) e^{\frac{K(l)}{16\pi}} I_0\left(\frac{K(l)}{8\pi}\right).$$

where l is the renormalized flow variable, I_0 and I_1 are modified Bessel functions, $y = e^{-E_c/k_B T}$ is the fugacity of dislocation pairs, and E_c is the dislocation core energy. The bare value of the Young's modulus $K(0)$ can be calculated from the strain fluctuations[41] in a defect-free solid, but with a fixed fraction of pinned particles, and is employed as the initial value for the renormalization recursion relationship. The core energy E_c can be calculated by measuring the probability density p_d to observe a dislocation pair per unit area using the expression[41]

$$p_d = \frac{16\sqrt{3}\pi^2}{K - 8\pi} I_0\left(\frac{K}{8\pi}\right)\exp\left(\frac{K}{8\pi}\right)\exp\left(\frac{-2E_c}{k_B T}\right). \tag{4}$$

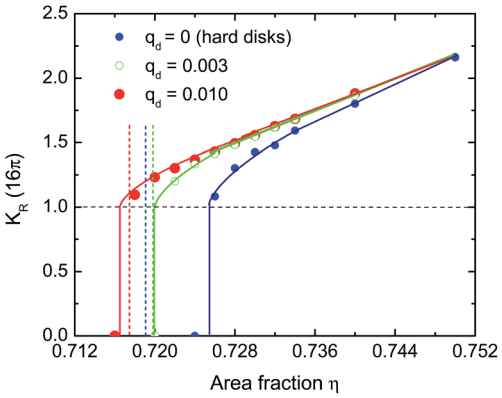

Fig. 5 Renormalized Young's modulus K_R as a function of area fraction η for pure hard disks without quenched disorder $q_d = 0$ (blue), and with pinning fractions $q_d = 0.003$ (green) and $q_d = 0.01$ (red). Dashed lines denote the solid binodal as obtained from the Maxwell construction to the equation of state.

The initial value of the fugacity $y(0)$ is equal to e^{-E_c/k_BT}. Using the initial values $y(0)$ and $K(0)$ in the renormalization recursion relationships, we can determine the thermodynamic values of K and y by taking the limit $l \to \infty$. Fig. 5 shows the renormalized Young's modulus $K_R = K(l \to \infty)$ as a function of area fraction η for pure hard disks, and for impurity fractions $q_d = 0.003$ and 0.01. For hard disks without any pinned particles, we find that the renormalized Young's modulus K_R changes from 16π to 0 at an area fraction $\eta = 0.724$, which is indicative of a KT type solid–hexatic transition. In addition, we find that the renormalized Young's modulus K_R increases with pinning fraction q_d, which means that the stiffness of the crystal increases by the presence of these pinned particles. We also determine the area fractions at which the solid–hexatic phase transition occurs using the melting criterion eqn (3), and we find good agreement with the area fraction values as obtained from the sub-block scaling analysis as shown in Fig. 4. Comparing the area fraction at which the solid–hexatic transition occurs with the coexisting densities as determined from the Maxwell constructions to the equations of state, we find that for $q_d > 0.003$ the KT solid–hexatic transition is preempted by a first-order liquid–solid phase transition. In addition, we plot the probability density p_d to find a dislocation pair per unit area as a function of area fraction η in Fig. 6(a). We observe that p_d decreases upon increasing the pinning fraction q_d. In addition, it was predicted by Chui that a first-order solid–liquid transition driven by the spontaneous proliferation of grain boundaries may preempt the solid–hexatic transition when the core energy E_c of a dislocation becomes less than 2.84 k_BT.[42] In Fig. 6(b), we show the dislocation core energy E_c as computed from p_d (eqn (4)) as a function of area fraction η, which shows that in the solid phase E_c always exceeds the critical value 2.84 k_BT. This result indicates that the first-order solid–liquid transition might not be induced by spontaneous proliferation of grain boundaries. Fig. 7 shows a typical configuration of the liquid–solid coexistence phase at $\eta = 0.694$ for $q_d = 0.01$. We clearly see from the above picture that most pinned particles are located at the crystalline region, whereas the five- and seven-fold defects are clustered far away from the pinned particles. This may indicate that the pinned particles act as a nucleation seed for crystallization.

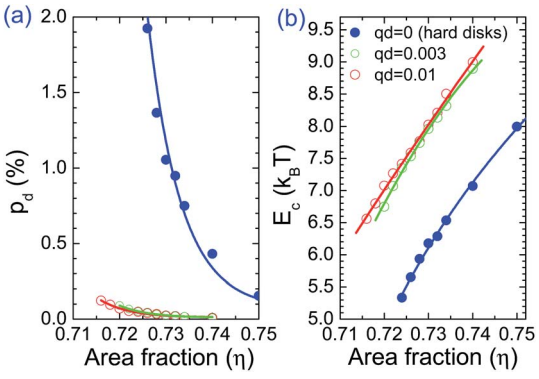

Fig. 6 (a) Probability density p_d of a dislocation pair per unit area as a function of area fraction η and (b) dislocation core energy E_c as a function of area fraction η for hard disks without quenched disorder $q_d = 0$ (blue), with pinning fractions $q_d = 0.003$ (green) and $q_d = 0.01$ (red). Lines are fits to the data.

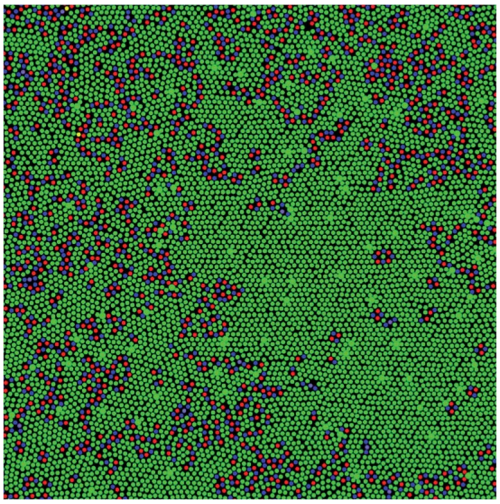

Fig. 7 Typical configuration of the liquid–solid coexistence phase at $\eta = 0.694$ for $q_d = 0.01$. We plot the size of pinned particles in 1.5σ just for visualization. Green particles are particles with six nearest neighbors, blue particles are 5-fold defects, red particles are 7-fold defects, yellow particles are 4-fold defects and grey particles are 8-fold defects.

V. Conclusions

In conclusion, we studied the effect of quenched disorder on the melting mechanism of 2D solids of hard disks by pinning randomly chosen particles on a triangular lattice. Using large-scale EDMD simulations, we observed that the two-stage melting scenario with an intermediate hexatic phase of a 2D system of hard disks[26,27] does *not* persist in the presence of pinned particles on a lattice. We showed that the hexatic phase is destabilized and that a first-order solid–liquid phase transition preempts the Kosterlitz–Thouless-type solid–hexatic

transition. These findings are corroborated with a renormalization group analysis based on the KTHNY theory, which shows that the renormalized Young's modulus of the crystal is increased by the presence of pinned particles. With regard to pinned particles at random sites, it was shown theoretically that the KTHNY melting scenario persists, and that the solid phase is destroyed entirely for high pinning fractions resulting in a hexatic glass.[33–37] Indeed, experiments and simulations on 2D melting of super-paramagnetic colloidal particles with quenched disorder confirmed the increased stability range of the hexatic phase.[38] Thus our results show that quenched disorder due to pinning of particles on a lattice leads to a different melting scenario than in the case of pinning at random positions. In the case of quenched disorder due to pinning on a lattice, the solid phase is stabilised, whereas pinning at random sites destabilizes the crystal. Although our results are obtained for a system of hard disks and it is supposed that the melting behavior in 2D is very sensitive to the precise interparticle interactions, it is tempting to speculate that the hexatic phase is also destabilized by pinning to an underlying crystalline lattice in a system of repulsive magnetic particles as studied in ref. 38 for sufficiently high pinning fractions. In this case, the stability of the solid phase can be studied as a function of Γ, which is related to the external magnetic field that controls the dipolar interactions between the particles.[38] For sufficiently high Γ, the particle interactions are sufficiently strong to stabilize a solid phase. Upon decreasing Γ, the melting behavior can be studied at a fixed fraction of particles pinned to a lattice both in simulations and experiments. The different pinning scenarios may be investigated in experiments on colloidal particles by using optical tweezers. We hope that our findings will stimulate research in this direction.

Acknowledgements

We gratefully acknowledge financial support from a NWO-Vici grant.

References

1 J. M. Kosterlitz and D. J. Thouless, *J. Phys. C: Solid State Phys.*, 1973, **6**, 1181.
2 D. R. Nelson and B. I. Halperin, *Phys. Rev. B: Solid State*, 1979, **19**, 2457.
3 A. P. Young, *Phys. Rev. B: Solid State*, 1979, **19**, 1855.
4 K. J. Strandburg, *Rev. Mod. Phys.*, 1988, **60**, 161.
5 J. G. Dash, *Rev. Mod. Phys.*, 1999, **71**, 1737.
6 U. Gasser, *J. Phys.: Condens. Matter*, 2009, **21**, 203101.
7 K. Zahn, R. Lenke and G. Maret, *Phys. Rev. Lett.*, 1999, **82**, 2721.
8 P. Karnchanaphanurach, B. Lin and S. A. Rice, *Phys. Rev. E: Stat. Phys., Plasmas, Fluids, Relat. Interdiscip. Top.*, 2000, **61**, 4036.
9 Y. Peng, Z. Wang, A. M. Alsayed, A. G. Yodh and Y. Han, *Phys. Rev. Lett.*, 2010, **104**, 205703.
10 Y. Han, N. Y. Ha, A. M. Alsayed and A. G. Yodh, *Phys. Rev. E: Stat., Nonlinear, Soft Matter Phys.*, 2008, **77**, 041406.
11 M. Mazars, arXiv:1301.1571, 2013.
12 S. C. Kapfer and W. Krauth, arXiv: 1406.7224, 2014.
13 B. J. Alder and T. E. Wainwright, *Phys. Rev.*, 1962, **127**, 359.
14 W. G. Hoover and F. H. Ree, *J. Chem. Phys.*, 1968, **49**, 3609.
15 J. Lee and K. J. Strandburg, *Phys. Rev. B: Condens. Matter Mater. Phys.*, 1992, **46**, 11190.
16 J. A. Zollweg and G. V. Chester, *Phys. Rev. B: Condens. Matter Mater. Phys.*, 1992, **46**, 11186.
17 H. Weber, D. Marx and K. Binder, *Phys. Rev. B: Condens. Matter Mater. Phys.*, 1995, **51**, 14636.
18 J. J. Alonso and J. F. Fernández, *Phys. Rev. E: Stat. Phys., Plasmas, Fluids, Relat. Interdiscip. Top.*, 1999, **59**, 2659.
19 H. Weber and D. Marx, *Europhys. Lett.*, 1994, **27**, 593.
20 J. F. Fernández, J. J. Alonso and J. Stankiewicz, *Phys. Rev. Lett.*, 1995, **75**, 3477.
21 A. C. Mitus, H. Weber and D. Marx, *Phys. Rev. E: Stat. Phys., Plasmas, Fluids, Relat. Interdiscip. Top.*, 1997, **55**, 6855.
22 J. F. Fernández, J. J. Alonso and J. Stankiewicz, *Phys. Rev. E: Stat. Phys., Plasmas, Fluids, Relat. Interdiscip. Top.*, 1997, **55**, 750.
23 A. Jaster, *Phys. Rev. E: Stat. Phys., Plasmas, Fluids, Relat. Interdiscip. Top.*, 1999, **59**, 2594.
24 C. H. Mak, *Phys. Rev. E: Stat., Nonlinear, Soft Matter Phys.*, 2006, **73**, 065104.
25 A. Jaster, *Phys. Lett. A*, 2004, **330**, 120.
26 E. P. Bernard and W. Krauth, *Phys. Rev. Lett.*, 2011, **107**, 155704.
27 M. Engel, J. A. Anderson, S. C. Glotzer, M. Isobe, E. P. Bernard and W. Krauth, *Phys. Rev. E: Stat., Nonlinear, Soft Matter Phys.*, 2013, **87**, 042134.
28 C. A. Murray and D. H. Van Winkle, *Phys. Rev. Lett.*, 1987, **58**, 1200.
29 S. A. Rice, *Chem. Phys. Lett.*, 2009, **479**, 1.
30 R. E. Kusner, J. A. Mann, J. Kerins and A. J. Dahm, *Phys. Rev. Lett.*, 1994a, **73**, 3113.
31 A. H. Marcus and S. A. Rice, *Phys. Rev. Lett.*, 1996, **77**, 2577.
32 W. Qi, A. P. Gantapara and M. Dijkstra, *Soft Matter*, 2014, **10**, 5449.
33 D. R. Nelson, *Phys. Rev. B: Condens. Matter Mater. Phys.*, 1983, **27**, 2902.
34 R. A. Serota, *Phys. Rev. B: Condens. Matter Mater. Phys.*, 1986, **33**, 3403.
35 R. E. Kusner, J. A. Mann and A. J. Dahm, *Phys. Rev. B: Condens. Matter Mater. Phys.*, 1994, **49**, 9190.
36 P. Yunker, Z. Zhang and A. G. Yodh, *Phys. Rev. Lett.*, 2010, **104**, 015701.
37 D. Carpentier and P. Le Doussal, *Phys. Rev. Lett.*, 1998, **81**, 1881.
38 S. Deutschländer, T. Horn, H. Löwen, G. Maret and P. Keim, *Phys. Rev. Lett.*, 2013, **111**, 098301.
39 J. E. Mayer and W. W. Wood, *J. Chem. Phys.*, 1965, **42**, 4268.
40 K. Bagchi, H. C. Andersen and W. Swope, *Phys. Rev. Lett.*, 1996, **76**, 255.
41 S. Sengupta, P. Nielaba and K. Binder, *Phys. Rev. E: Stat. Phys., Plasmas, Fluids, Relat. Interdiscip. Top.*, 2000, **61**, 6294.
42 S. T. Chui, *Phys. Rev. Lett.*, 1982, **48**, 933.

